Sea-surface temperature and dynamic height distributions in the central tropical South Atlantic Ocean

Tropical South Atlantic Ocean
Sea-surface temperature
Geostrophic currents
Seasonal cycle

Océan Atlantique Sud tropical
Température de surface
Courant géostrophique
Cycle saisonnier

R. L. Molinari *
National Oceanic and Atmospheric Administration, Atlantic Oceanographic and Meteorological Laboratories, 4301 Rickenbacker Causeway, Miami, Florida 33149, U.S.A.
* Prepared while visiting scientist at: Muséum National d'Histoire Naturelle, Laboratoire d'Océanographie Physique, Laboratoire associé au CNRS n° 175, 43-45, rue Cuvier, 75231 Paris Cedex 05, France.

Received 29/3/82, in revised form 1/7/82, accepted 27/7/82.

ABSTRACT

Dynamic height and temperature observations collected during four cruises to the central tropical South Atlantic Ocean are presented. The dynamic topographies of the sea-surface along sections extending from 1°N to 9°S during two different austral summer and two different austral winter cruises are similar to topographies given earlier. They support the contention of Katz (1981) that the dynamic relief of the sea-surface in the Atlantic varies in phase with changes in the surface wind stress field. Synoptic and climatological sea-surface temperature (SST) distributions during early austral winter (June-July) are more symmetric with respect to the equator than SST distributions later in austral winter (August-September). Comparison of the observations with results from various numerical modelling efforts suggests that the early winter pattern may represent an ocean response to an increase in zonal winds, while the late winter pattern may include an additional response to an increase of meridional winds.

Oceanol. Acta, 1983, **6**, 1, 29-34.

RÉSUMÉ

Répartitions de la température de surface et de la hauteur dynamique au centre de l'Océan tropical Atlantique Sud.

Des observations de hauteur dynamique et de température ont été effectuées au cours de quatre campagnes au centre de la partie tropicale de l'Océan Atlantique Sud. Pendant deux étés et deux hivers de l'hémisphère austral, la topographie dynamique de la surface le long de sections méridiennes, entre 1°N et 9°S, est semblable aux topographies observées précédemment, ce qui confirme le résultat de Katz (1981), selon lequel les variations annuelles du relief dynamique de la surface de l'Atlantique central sont en phase avec celles du champ de tension du vent.
Les répartitions synoptiques et climatologiques de la température de surface présentent une symétrie par rapport à l'équateur qui est plus marquée au début de l'hiver austral (juin-juillet) que plus tard dans cette saison (août-septembre).
La comparaison des observations avec les résultats de différents modèles numériques suggère qu'au début de l'hiver, l'océan répond à un renforcement des vents zonaux, tandis qu'à la fin de l'hiver, il répond aussi à un renforcement des vents méridiens.

Oceanol. Acta, 1983, **6**, 1, 29-34.

INTRODUCTION

South of the equator, in both the Atlantic and Pacific Oceans, a tongue of cold water extends from the eastern boundary to the central basin during austral winter, but not austral summer (Hastenrath, Lamb, 1977; hereinafter referred to as HL). In the Atlantic, the tongue extends farthest west during the months of August and September. The tongue plays an important role in local air-sea energy fluxes and the global energy balance (Hastenrath, 1980).

Several surface currents have been identified in the region of the cold water tongue. The South Equatorial Current (SEC) flows to the west in several branches located between 15°S and somewhat north of the equator. The branches of the SEC are separated by eastward flows. The South Equatorial Undercurrent (SEUC) is a subsurface eastward flow, typically located between 3 and 5°S, which can "surface" resulting in eastward surface flow (Molinari *et al.*, 1981, for instance). The South Equatorial Countercurrent (SECC) is a surface eastward flow located between 7 and 9°S (Molinari, 1982). Katz (1981) proposed an annual cycle for the dynamic topography of the sea-surface between 10°S and 10°N, which implies an annual cycle in the intensity of the associated geostrophic currents. The SEC should be most intense during austral winter according to Katz (1981). Few data are available to study the relation of these surface currents to the surface temperature distribution.

Four cruises were made to the central tropical South Atlantic Ocean during 1978, 1979, and 1980. Temperature, salinity and direct current observations were obtained during two austral summer and two austral winter cruises. Dynamic topographies of the sea-surface along several meridional sections are described and compared to the earlier observations of Katz (1981). Sea-surface temperature (SST) and near-surface temperature distributions are described and compared to climatological distributions. Finally, the synoptic and climatological SST distributions and results from numerical models are used to suggest possible relations between the wind, current and temperature fields.

DYNAMIC TOPOGRAPHY OF THE SEA-SURFACE

The data collected during July-August 1978, January-February 1979, July 1979 and February-March 1980 are listed in Molinari *et al.* (1979) and Roffer *et al.* (1981). Data analysis techniques are also listed in these reports. Observational and computational uncertainties are given in Molinari *et al.* (1981) and Molinari (1982).

Katz (1981), using Merle's (1978) mean annual dynamic topography of the sea-surface, identifies two troughs and one ridge along a meridional section in the tropical South Atlantic. The equatorial trough is located between 0° and 2°S, the south equatorial ridge between about 5 and 7°S and another trough at about 13°S.

Dynamic height sections of the sea-surface computed relative to 1000 m are given in Figure 1. Dynamic

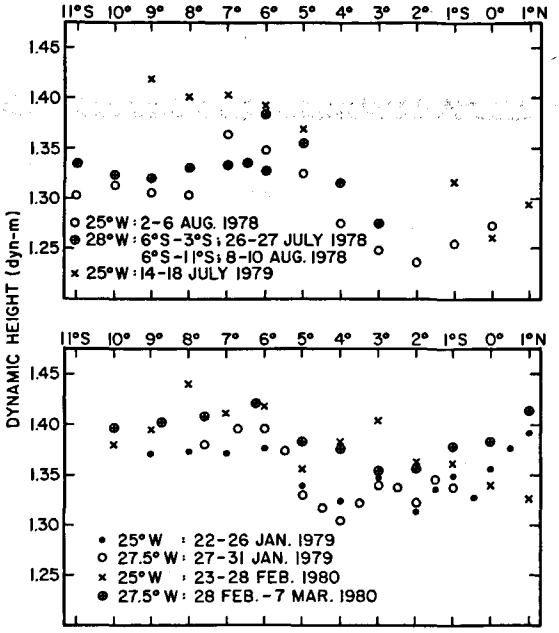

Figure 1

Dynamic height (dyn-m) sections of the sea-surface relative to 1000 m. Upper panel sections were obtained during austral winter and lower panel sections during austral summer.

height differences between the equatorial trough and south equatorial ridge obtained during these cruises and those computed by Katz (1981) are given in the Table. Following Katz (1981), the differences are obtained by first averaging the two highest dynamic height values on the ridge and the two lowest values in the trough and then subtracting. The austral winter differences observed during 1978 and 1979 are quite similar to those given by Katz (1981). The austral summer differences are somewhat higher than those of Katz (1981), but they are consistently lower than the winter values.

On three of the four austral summer sections, a secondary ridge is observed at 3°S. Although the dynamic relief of the ridge is only about 3 dyn-cm (Fig. 1), because of its proximity to the equator eastward geostrophic surface speeds associated with the southern flank of the feature range from 10 to 30 cm/sec. The eastward surface flow occurs above the SEUC and represents "surfacing" of this subsurface feature (Molinari, 1982).

Table

Dynamic height differences (dyn-cm) between the equatorial trough and south equatorial ridge observed during the four synoptic cruises and average differences given for two seasons by Katz (1981). The standard error of the mean computed by Katz (1981) is also given.

Section	Date	Dynamic height difference (dyn-cm)
25°W	1-6 August 1978	11.1
25°W	14-18 July 1979	13.5
Katz (1981)	July-September	11.9 (1.0)
25°W	22-26 January 1979	5.4
25°W	23-28 February 1980	9.7
27.5°W	28 February-27 March 1980	6.0
Katz (1981)	February-April	2.3 (1.6)

The data are inadequate to define the properties of the southern trough. However, a poleward drop in dynamic height values is indicated south of 7°S in most of the sections, suggestive of an eastward surface geostrophic flow, the SECC.

TEMPERATURE DISTRIBUTIONS

SST distributions are given in Figures 2 and 3. Isotherms taken from the mean monthly SST charts of HL are also displayed in these figures. In general, the large-scale synoptic SST distributions are very similar to the large-scale climatological distributions.

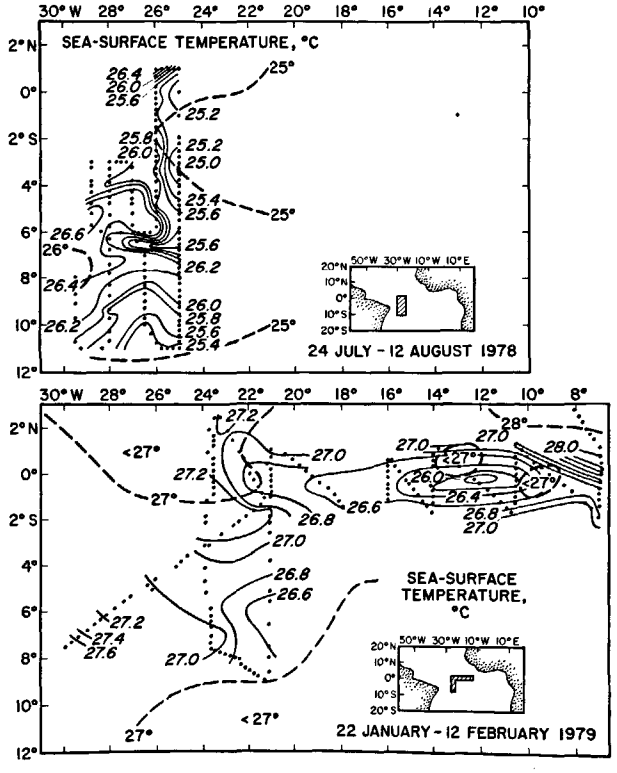

Figure 2

Sea-surface temperature, SST (°C) distributions for the time periods given. Dots represent data points. Dashed lines represent isotherms taken visually from the August SST chart of HL, upper panel, and from the January SST chart, lower panel.

Regions of relatively colder water are observed on or near the equator during both seasons. However, there are distinct seasonal differences in the structure of the cold water tongue. During austral winter, the cold water extends as a continuous tongue from the eastern to central basin (HL and Fig. 3). The 25°C isotherm from the August chart of HL indicates colder water extends over a larger area during this month than during July. The austral winter 1978 data were collected primarily in August, while the winter 1979 data in July. The larger area of colder water observed during the former cruise is consistent with the climatological distributions.

In contrast, during austral summer 1979, the cold water is located within an isolated patch centered at about 16°W, just south of the equator (Fig. 2). A similar patch can be inferred from the austral summer 1980 SST distributions (Fig. 3). The HL SST chart for

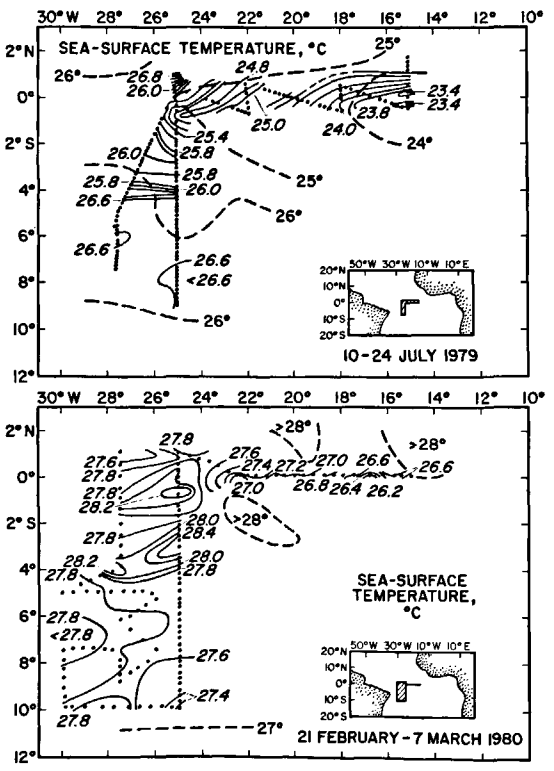

Figure 3

Sea-surface temperature, SST (°C) distributions for the time periods given. Dots represent data points. Dashed lines represent isotherms taken visually from the July SST chart of HL, upper panel, and from the February SST chart, lower panel.

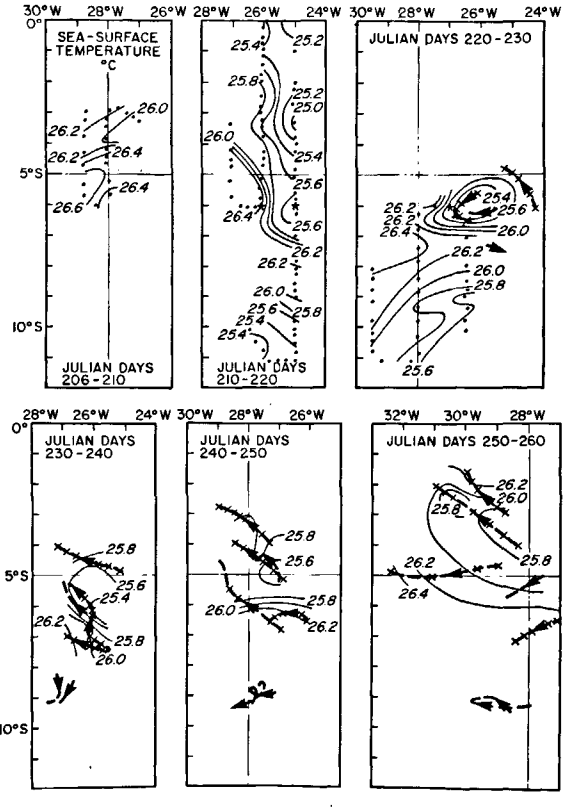

Figure 4

Sea-surface temperature (°C) distributions derived from drifting buoy (crosses) and ship (dots) observations for ten-day periods (Julian day 206=25 July 1978). Ten-day long drifting buoy trajectories are also given. Station positions for vertical temperature profiles given in Figure 5 are indicated.

February shows isolated patches of somewhat colder water in the same area.

Satellite tracked drifting buoys were deployed during the 1978 cruise. Several of the buoys were equipped with SST sensors which provide data to look at SST evolution over a two-month period. It should be noted that the buoy temperature data and trajectories do not provide sufficient data to perform quantitative near surface heat budget computations for two reasons. First, over long periods of time, buoy trajectories do not represent distinct water parcel trajectories because of windage effects on the surface elements of the buoys. Second, SST is not a conservative property and additional data are not available to determine surface heat fluxes. However, these data are sufficiently accurate to use with ship data to construct ten-day average charts of SST distribution.

Initially, temperatures west of 28°W were higher than 26°C (Fig. 4). Temperatures less than 25.8°C were observed during the first 14 days east of 26°W between 3 and 7°S. By days 250 to 260, waters colder than 25.8°C were observed west of 28°W and north of 5°S. Several mechanisms could be responsible for this cooling, upward movement of the thermocline and subsequent upwelling, deepening of the mixed layer and subsequent entrainment of colder water and/or advection.

Several subsurface temperature profiles collected during austral winter 1978 are given in Figure 5. The profile at 6°S, 25°W was obtained on Julian day 217, the profile at 6°S, 26°W was obtained on Julian day 211, and the profile at 6°S, 27°W on Julian day 221. The positions of the profiles relative to the SST field are shown in Figure 4. Lower temperatures are observed further to the west than previously at the time of this last profile. The profiles in the cooler water are characterized by deeper mixed layers, 85 m versus 65 m, and deeper thermoclines than the warmer water profile. The former profiles appear very similar.

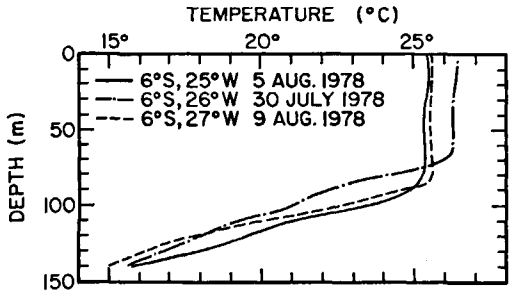

Figure 5
Vertical temperature profiles, station positions are given in Figure 4.

Vertical temperature gradients within the thermocline are very large between the 17.5 and 22.5°C isotherms (Fig. 5). These isotherms will be used to display cruise-to-cruise differences in thermocline depth. During the two austral summer cruises, the equatorial thermocline is relatively flat (Fig. 6). At 15°W on the equator, the austral winter thermocline is some 20 to 30 m higher than during either summer cruise. West of

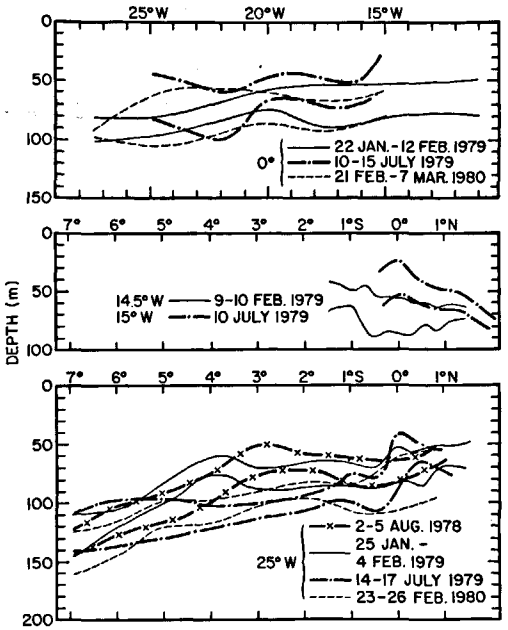

Figure 6
The 17.5 and 22.5°C isotherms, from the time periods indicated, taken to represent the boundaries of the core of the thermocline along the equator (upper panel), along 14.5/15°W (middle panel) and along 25°W (bottom panel).

about 21°W, there is little difference in thermocline depth. These findings are consistent with the climatological representations of the depth of the equatorial thermocline given by Merle (1980).

Cross-equatorial thermocline sections at 14.5/15 and 25°W are also given in Figure 6. At the eastern section, as described above, the austral winter 1979 thermocline on the equator is some 30 m shallower than the summer 1979 thermocline. At 1.5°N, the difference is only about 10 m. At 25°W, there is little difference between the austral winter 1978 and summer 1979 thermocline sections. The austral winter 1979 thermocline is deeper than the other thermoclines between about 2 and 4°S but is shallowest of all thermoclines at the equator. The two summer thermoclines have a similar meridional structure.

DISCUSSION

The dynamic height sections given in Figure 1 provide additional data to support the finding of Katz (1981) that the dynamic topography of the central Atlantic sea-surface varies in phase with the annual cycle of wind stress. In particular, largest relief between the equatorial trough and south equatorial ridge is observed during austral winter, when climatological winds are strongest, HL. The sea-surface topography has less relief in austral summer when winds are weaker. In addition, a secondary ridge was observed at 3°S on several of the austral summer sections. These results imply that the geostrophic component of the SEC is strongest during the austral winter and that a surface eastward flow may divide a weaker SEC into two

branches during austral summer. However, as noted by Katz (1981), the actual configuration of surface currents can be different because of possible direct wind forcing effects.

Figure 7 shows several schematic mean monthly SST distributions taken from HL. The changes in SST patterns between May and June are dramatic, with the sudden appearance of a large area of temperatures less than 25°C. West of 10°W, the cold water tongue appears more symmetric about the equator during June, than during September. In fact, by August (not shown) and through September, the 25 and 26°C are observed at approximately the same longitudes at the equator and 5°S. Similarly in the synoptic distributions, at 25°W, colder waters are observed further south during August 1978 than during July 1979.

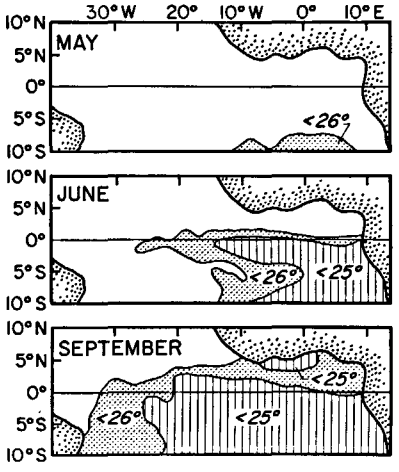

Figure 7

Schematic diagrams representing mean monthly sea-surface temperature distributions for May, June and September derived from the charts of HL.

Numerical models used to explain the evolution of the SST field and thermocline depth are typically driven by the wind stress. The model results can be compared to the observations to develop a qualitative description of those processes active in the development of the SST field. Before making this comparison, a brief discussion of some wind data collected in the region is given.

At about 30°W, near the equator, Katz *et al.* (1981) analyzed synoptic data which indicate that the zonal component of the wind increased some 4 m/sec. and the meridional component some 2 m/sec. during May 1979. The relaxation of the wind observed between February and April 1979 and after December 1979 did not occur as rapidly. Climatological data suggest that a similar temporal evolution is typical of the central Atlantic, HL. Thus between the austral summer 1979 and austral winter 1979 cruises both components of the wind have increased dramatically.

Philander and Pacanowski (1980) consider the response of an equatorial ocean to a sudden onset of a westward zonal wind stress. In their results, the thermocline deepens in the west and rises in the east. The response is symmetric about the equator. The winds also cause horizontal divergence on the equator which induces equatorial upwelling. The resulting SST distribution is also symmetric about the equator. Between austral summer and winter 1979, the thermocline rose some 20 to 30 m at 15°W (Fig. 6) as it does in the climatological representations of Merle (1980). Although the synoptic data are not conclusive, the initial thermocline response does appear to be symmetric about the equator at 15 and 25°W (Fig. 6). The early austral winter HL distributions (Fig. 7) and the July 1979 SST distribution (Fig. 3) show a cold water tongue which remains closer to the equator than later in the winter (Fig. 2 and 7). Thus, the initial structure of the cold water tongue is similar to the response predicted by a model driven by the sudden onset of the zonal wind stress component.

In another numerical model, Philander and Pacanowski (1981) drive an ocean with only a southerly wind stress component. An area of coastal upwelling is generated on the eastern boundary. The upwelled water is advected west, south of the equator, by Ekman drift and Rossby wave propagation. The SST distribution predicted by this model is very similar to the HL distribution for September (Fig. 7) and the austral winter 1978 distribution (Fig. 2) in that the cold water is observed considerably further south than earlier in the austral winter. The dynamic height sections (Fig. 1) indicate that the geostrophic component of the SEC is most intense during the winter. The drifting buoy trajectories all indicate net westward drift in the vicinity of the cooler water (Fig. 4). Thus, as in the model, advection can play a role in the westward propagation of the cooler water south of the equator.

However, somewhat deeper mixed layers occur coincidentally with the lower temperatures (Fig. 4). Thus, it is possible that increased winds caused deepening of the mixed layer and subsequent entrainment of colder water. Insufficient wind data exist to quantify the possible effect of entrainment.

When the surface winds relax in a zonal stress model, the thermocline rises in the west and sinks in the east (Cane, 1980). The thermocline has deepened east of 21°W between austral winter 1979 and summer 1980, after the winds relaxed. When the winds relax in the meridional stress model, the cold water tongue contracts to the east, partially in response to surfacing of a subsurface current originally generated by the onset of the meridional stress. These similarities between the observations and model results suggest that the SST distribution responds to relaxations in both the zonal and meridional wind components.

In the region of the cold water patch observed at 16°W during austral summer 1979 (Fig. 2), the thermocline and the associated colder waters are observed closer to the surface at 20°W than further west (Fig. 6). Thus, the surface patch may represent surfacing of the EUC, a remanent of cold water from the previous winter and/or a local upwelling event. Since similar patches appear on the HL charts, they may represent a permanent feature of the austral summer SST field.

Acknowledgements

The outstanding efforts of the officers and crew of the NOAA Ship Researcher are gratefully acknowledged. Portions of this work were funded by the Centre National de la Recherche Scientifique of France, the Department of Energy and the NOAA Special Research Programs Office.

REFERENCES

Cane M. A., 1980. On the dynamics of equatorial currents, with application to the Indian Ocean, *Deep-Sea Res.*, **27**, 525-544.

Hastenrath S., 1980. Heat budget of tropical ocean and atmosphere, *J. Phys. Oceanogr.*, **10**, 159-170.

Hastenrath S., Lamb P., 1977. *Climatic atlas of the tropical Atlantic and Eastern Pacific Oceans*, University of Wisconsin Press, 105 p.

Katz E. J., 1981. Dynamic topography of the sea surface in the equatorial Atlantic, *J. Mar. Res.*, **39**, 53-63.

Katz E. J., Molinari R. L., Cartwright D. E., Hisard P., Lass H. U., de Mesquita A., 1981. The seasonal transport of the Equatorial Undercurrent in the Western Atlantic (during FGGE), *Oceanol. Acta*, **4**, 4, 445-450.

Merle J., 1978. Atlas hydrologique saisonnier de l'océan Atlantique intertropical, *Trav. Doc. ORSTOM*, **82**, 184 p.

Merle J., 1980. Seasonal heat budget in the equatorial Atlantic Ocean, *J. Phys. Oceanogr.*, **10**, 464-469.

Molinari R. L., 1982. Observations of eastward currents in the tropical South Atlantic Ocean: 1978-1980, submitted to *J. Geophys. Res.*

Molinari R. L., Hazelworth J. B., Ortman D. A., 1979. Data from OTEC site characterization studies in the Gulf of Mexico and tropical South Atlantic, NOAA Tech. Mem. ERL AOML-39.

Molinari R. L., Voituriez B., Duncan P., 1981. Observations in the subthermocline undercurrent of the equatorial South Atlantic Ocean: 1978-1980, *Oceanol. Acta*, **4**, 4, 451-456.

Philander S. G. H., Pacanowski R. C., 1980. The generation of equatorial currents, *J. Geophys. Res.*, **85**, 1123-1136.

Philander S. G. H., Pacanowski R. C., 1981. The oceanic response to cross-equatorial winds (with applications to coastal upwelling in low-latitudes), *Tellus*, **33**, 201-210.

Roffer C., Callery K., Pazos M. C., Molinari R. L., 1981. Data from OTEC site characterization studies in the tropical South Atlantic, NOAA Tech. Mem. ERL AOML-47.